P-ISSN: 2723-3863 E-ISSN: 2723-3871 Vol. 6, No. 5, October 2025, Page. 3153-3172

https://jutif.if.unsoed.ac.id

DOI: https://doi.org/10.52436/1.jutif.2025.6.5.5179

Image-Based Classification of Rice Field Conversion: A Comparison Between MLP and SVM Using Multispectral Features

Anisya*1, Sumijan2, Anna Syahrani3

^{1,3}Department of Informatics Engineering, Faculty of Engineering, Padang Institute of Technology, Indonesia

²Department of Information System, Faculty of Computer Science, University of Putra Indonesia "YPTK", Indonesia

Email: ¹anisya@itp.ac.id

Received: Jul 27, 2025; Revised: Sep 1, 2025; Accepted: Sep 2, 2025; Published: Oct 16, 2025

Abstract

The conversion of farmland into non-agricultural purposes has emerged as a pressing concern in many urban regions, including Koto Tangah District, Padang City. In this area, agricultural land experienced a 4% shift in land use between 2022 and 2024. If this trend continues, it could lead to a notable decline in rice production and ultimately threaten food security. This research focuses on examining spatial transformations of rice fields from 2022 to 2024 by utilizing Sentinel-2 satellite imagery along with advanced classification techniques. Vegetation and moisture features were extracted using NDVI, NDWI, texture analysis through GLCM, and Principal Component Analysis (PCA). To classify land cover changes and assess model accuracy, two machine learning approaches were applied: Multilayer Perceptron (MLP) and Support Vector Machine (SVM). The findings reveal a considerable reduction in dense vegetation, indicated by the downward shift of NDVI values in 2024. MLP achieved an accuracy of 82%, outperforming SVM, which reached 71%. Furthermore, MLP obtained a higher F1-score for non-rice field detection (0.75 vs. 0.74) and produced more realistic delineations of rice field boundaries during spatial validation. These outcomes highlight the potential of MLP in monitoring land use conversion, supporting agricultural land conservation, and guiding sustainable urban planning. Moreover, the study contributes to computer science by advancing the use of machine learning for spatio-temporal analysis and reinforcing the role of non-linear models in satellite image classification.

Keywords: Land Use Change, Machine Learning, Multilayer Perceptron (MLP), Multispectral Remote Sensing, Rice Field Conversion, Support Vector Machine (SVM)

This work is an open access article and licensed under a Creative Commons Attribution-Non Commercial
4.0 International License



1. INTRODUCTION

Koto Tangah District in Padang City encompasses a relatively large agricultural area and serves as one of the region's key agricultural sectors [1]. However, in recent years, the district has experienced a notable reduction in rice paddy land due to land conversion. Based on statistical records, the area of rice paddies declined from 36.219,80 hectares in 2019 to 26.196,06 hectares in 2023 [2]. This downward trend indicates a land-use shift that warrants serious concern, as it directly affects food security. The reduction of paddy fields inevitably impacts rice production. With an average yield of 5.2 tons per hectare per season [2], the loss of approximately 60 hectares conversion into a reduction of several hundred tons of rice annually [3]. This situation is increasingly alarming given the rising population and growing national demand for staple food [4].

The primary factor driving this decline is land conversion for development purposes, including residential housing, infrastructure, and commercial areas [5]. This phenomenon is consistent with international findings for instance, Oakleaf reported that agrarian ecosystems are particularly vulnerable to conversion pressures [3]. In China, for example, the proportion of cultivated land decreased from

https://jutif.if.unsoed.ac.id DOI: https://doi.org/10.52436/1.jutif.2025.6.5.5179

Vol. 6, No. 5, October 2025, Page. 3153-3172

59.75% in 1990 to 50.21% in 2020 [6]. Other studies also reveal that land with high ecological value is being converted at an accelerating rate for construction activities [7] [8] [9].

The Indonesian government has taken steps to address this challenge through various legal frameworks. Law Number 41 of 2009 concerning the Protection of Sustainable Food Agricultural Land (PLP2B) serves as the primary legal foundation to safeguard paddy fields from conversion pressures [10]. At the local level, the Padang City Government established a Regional Spatial Plan (RTRW) and issued Mayoral Regulation Number 20 of 2015 on the Optimization of Vacant Land Utilization. These policies aim to ensure sustainable land management and strengthen regional food security.

Within this context, a method capable of providing real-time and spatially explicit monitoring of land-use change is essential. Remote sensing technology offers an effective solution for periodically and comprehensively tracking land-use dynamics. Satellite imagery, such as Sentinel-2, which delivers multispectral data at a 10-meter spatial resolution, enables detailed analysis of vegetation conditions and land-cover changes. Vegetation indices, such as the Normalized Difference Vegetation Index (NDVI) and the Normalized Difference Water Index (NDWI) derived from combinations of red (B4), nearinfrared (B8), green (B3), and blue (B2) bands [11], have been extensively applied to detect paddy field changes and soil moisture variations [12].

Nevertheless, while remote sensing provides rich quantitative data, its interpretation requires advanced classification methods [13]. Major challenges arise from spatial complexity and the non-linear relationships between variables, which conventional algorithms often fail to capture effectively [14]. To address this gap, the present study developed an artificial intelligence-based approach using the Multilayer Perceptron (MLP) algorithm as the primary tool for classifying paddy field changes based on Sentinel-2 imagery during the 2022–2024 period.

MLP is a type of artificial neural network that operates through interconnected neurons arranged in multiple hidden layers [15]. It has proven effective in identifying hidden patterns within data characterized by complex and non-linear structures [16]. One of MLP's main advantages lies in its capacity for optimization through hyperparameter tuning techniques, such as GridSearchCV, which allow systematic improvement of model performance [17].

As part of model evaluation, this study also compared the classification outcomes of MLP with those generated by the Support Vector Machine (SVM) algorithm. SVM, a margin-based machine learning method, is widely used in image classification tasks [18] because of its effectiveness in handling high-dimensional data [19]. Guido [20] noted that SVM can deliver relatively stable classification accuracy even when training data are limited, provided that the classes are well-separated. However, its main limitations are reduced flexibility in modeling complex spatial structures [21] and the inability to account for spatial relationships between pixels an important consideration in remote sensing applications [22].

While many prior studies have employed vegetation indices and conventional classifiers such as SVM for land-use change detection, these methods still struggle to effectively capture spatial complexity and non-linear relationships among features [23]. This often leads to reduced classification accuracy, particularly in transitional zones between active and inactive rice fields. Similarly, Ricardo highlighted that several studies rely exclusively on basic spectral features, overlooking the integration of texture information or dimensionality reduction techniques that could enhance data representation [24]. To overcome these limitations, the present study integrates Sentinel-2 multispectral data with NDVI, NDWI, GLCM-based texture features, and PCA, before applying MLP as a more adaptive, non-linear model capable of capturing spatiotemporal variations. By comparing its performance with SVM, this research aims to advance the application of machine learning in satellite image classification and to provide a more accurate and practical model for monitoring rice field conversion.

DOI: https://doi.org/10.52436/1.jutif.2025.6.5.5179

P-ISSN: 2723-3863 E-ISSN: 2723-3871

Through this comparative analysis, the study seeks not only to map and assess rice field changes in Koto Tangah District but also to identify the most effective classification method for detecting landuse changes using multispectral satellite imagery. In summary, the objectives of this study are: (1) to analyze spatial changes in rice fields in Koto Tangah District for the 2022–2024 period using Sentinel-2 imagery, (2) to apply and evaluate the MLP algorithm in the classification of rice field changes based on remote sensing features, and (3) to compare the classification performance of MLP and SVM in order to determine the most suitable approach for spatial analysis.

2. METHOD

2.1. Study Area and Dataset

This study was carried out in Padang City, a major rice-producing region in West Sumatra Province, as illustrated in Figure 1. The figure presents the study area on a map, highlighting the designated region with a total coverage of 232.25 km². The primary data used were Sentinel-2 Level-1C satellite images with a spatial resolution of 10 meters, downloaded from the Google Earth Engine (GEE) platform for three time periods 2022, 2023, and 2024, to detect temporal changes in rice fields. The main dataset consisted of Sentinel-2 multispectral imagery in GeoTIFF format, complemented by shapefile data representing administrative boundaries and masking areas. Demographic data for the study area were used solely as supporting information. Land cover was classified into five categories: Built-up Land, Open Land, Mangrove Vegetation, Non-Mangrove Vegetation, and Water Bodies.

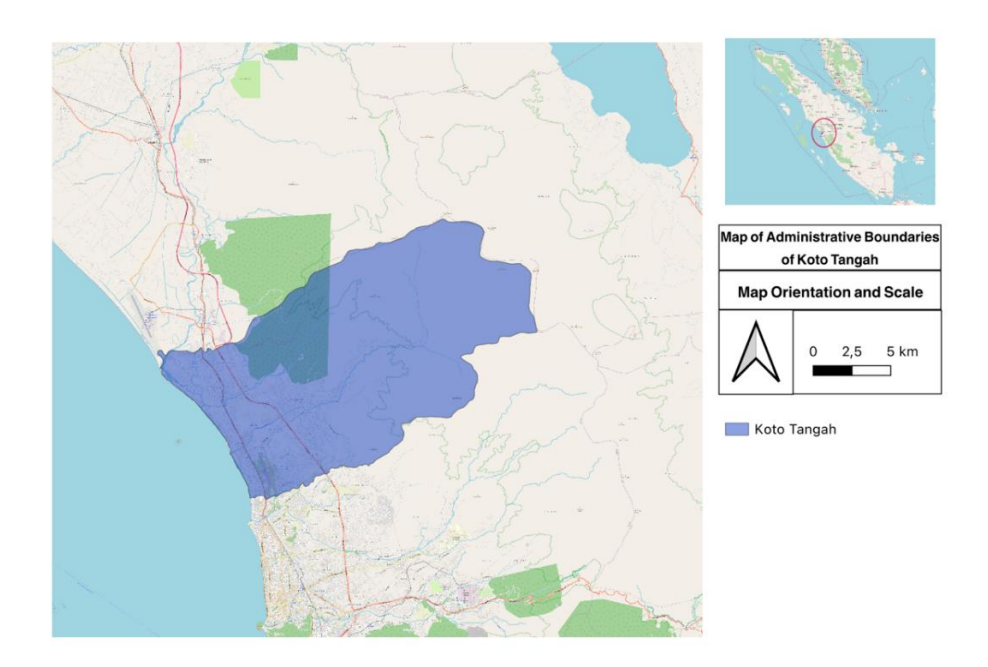


Figure 1. Administrative Boundaries of Koto Tangah District

In this study, a series of steps were undertaken to analyze land-use changes and evaluate the performance of two machine learning algorithms in managing non-linear spatial data, as shown in Figure 2. The rice field classification methodology began with data acquisition, followed by preprocessing tasks such as atmospheric correction, cloud masking, and image compositing. Subsequently, feature extraction was carried out using vegetation and water indices, texture analysis, and dimensionality reduction techniques. These extracted features served as inputs for the classification stage, where the Multilayer Perceptron (MLP) and Support Vector Machine (SVM) algorithms were implemented

E-ISSN: 2723-3871

https://jutif.if.unsoed.ac.id

DOI: https://doi.org/10.52436/1.jutif.2025.6.5.5179

Finally, performance evaluation and spatial validation were conducted to assess the accuracy and robustness of the classification outcomes.



Figure 2. The Methodology for Rice Field Classification

2.2. Data Preprocessing

The data pre-processing stage is a crucial initial step to ensure the quality of remote sensing imagery prior to classification and analysis [25]. This stage aims to eliminate atmospheric and cloudrelated distortions and to standardize the data spatially and temporally. In this study, several preprocessing procedures were applied to the Sentinel-2 imagery accessed via Google Earth Engine (GEE), including Atmospheric Correction with Sen2Cor. Atmospheric correction involves removing atmospheric effects such as gases, aerosols, and water vapor that can distort surface reflectance values [26]. Sentinel-2 Level-1C imagery available in GEE contains top-of-atmosphere (TOA) reflectance values, which do not accurately represent actual surface conditions [27]. Therefore, the imagery was converted to Level-2A (bottom-of-atmosphere/BOA) using the Sen2Cor algorithm, a physically based atmospheric correction module developed by the European Space Agency (ESA) [28]. This conversion results in images with corrected surface reflectance values, making them suitable for quantitative analysis [29]. In Next step, Cloud Masking using Band QA60, Clouds and their shadows pose a significant challenge in optical image analysis, as they introduce noise and reduce classification accuracy [30]. To address this issue, a cloud masking technique was implemented using the QA60 band, a quality assessment band provided in Sentinel-2 products, which detects pixels affected by clouds and other atmospheric artifacts [31]. The maskClouds() function was utilized to automatically detect and exclude pixels affected by clouds and shadows, ensuring that only cloud-free and relevant image regions were preserved for subsequent analysis [32]. Followed by Compiling Median Composite Images per Year, to achieve a stable representation of land conditions and mitigate seasonal variability, median composite images were generated for each observation year: 2022, 2023, and 2024. These composite images were derived from all available Sentinel-2 scenes in each year after cloud masking. The median compositing technique reduces temporary fluctuations caused by weather or atmospheric conditions and provides a statistically consistent representation of surface features [33]. This method also minimizes bias that can occur from selecting a single scene for analysis [34]. After the composite imagery was compiled, the next step was to clip the study area to include only the administrative boundaries of Koto Tangah District. This process was performed using a shapefile representing the district's administrative extent. Clipping the study area ensures that the entire classification and spatial analysis processes are focused solely on areas relevant to the research objectives, while also reducing unnecessary computational load [35].

2.3. Feature Extraction

The feature extraction stage is a critical process in satellite imagery-based classification systems, as it directly influences the quality of information used for model training and prediction [36]. In this study, features were extracted from Sentinel-2 imagery to represent land characteristics such as

P-ISSN: 2723-3863 E-ISSN: 2723-3871

vegetation, moisture, surface texture, and spectral components. These features were designed to capture spatial and spectral variations relevant to detecting changes in rice fields. The extracted features include Normalized Difference Vegetation Index (NDVI), Normalized Difference Water Index (NDWI), Gray Level Co-occurrence Matrix (GLCM) Texture Features.

NDVI is the most widely used vegetation index for monitoring vegetation cover and land productivity [37]. It is calculated based on the ratio of spectral reflectance values in the Near-Infrared (B8) and Red (B4) bands [38] as shown in Equation (1).

$$NDVI = \frac{(B8 - B4)}{(B8 + B4)} \tag{1}$$

NDVI values range from -1 to +1, with higher values indicating healthier and denser vegetation [39]. NDVI is particularly relevant in agricultural applications, as it can reflect plant growth phases, canopy density, and vegetation changes resulting from land use transformations [40]. In this study, NDVI was used to identify active rice field areas and detect changes in growth intensity [41].

NDWI is used to detect the presence of water or moisture on the land surface, an important indicator in rice field analysis [42], particularly in the early stages of planting and irrigation. It is computed using the spectral ratio between the Green (B3) and Near-Infrared (B8) bands, as shown in Equation (2).

$$NDWI = \frac{(B3 - B8)}{(B3 + B8)} \tag{2}$$

NDWI is effective in distinguishing wetlands or flooded areas from dry surfaces and is often used to identify newly plowed, recently planted, or water-saturated rice fields [43]. When combined with NDVI, NDWI can enhance the accuracy of active rice field classification.

In addition to spectral features, this study also incorporated texture features derived from the Gray Level Co-occurrence Matrix (GLCM) to capture spatial patterns and structures of the land surface. Texture images were generated from the NDVI channel by calculating a spatial gray-level correlation matrix and extracting several key statistical descriptors, (a) Contrast, which measures the intensity of local variation. High contrast typically appears at the edges of rice fields or in transitional land cover zones, (b) Homogeneity, which assesses the uniformity of pixel values. High homogeneity indicates a smooth, consistent texture, such as regularly planted rice fields, (c) Entropy, which quantifies the complexity or randomness of texture. High entropy reflects a high diversity of pixel values, often found in mixed or transitional land areas [44]. These GLCM-based texture features complement NDVI and NDWI by providing additional spatial context, thereby improving classification accuracy in areas with similar spectral characteristics but differing spatial structures [45].

To reduce redundancy and correlation among features and lower data dimensionality without losing critical information, Principal Component Analysis (PCA) was applied. PCA is a linear transformation technique that converts the original correlated variables into a new set of uncorrelated variables called principal components [46]. In this study, PCA was applied to four Sentinel-2 spectral bands (B2, B3, B4, B8) along with the NDVI and NDWI indices. The first three components (PC1–PC3) were used as additional features for classification. PCA helps minimize the risk of model overfitting and accelerates the training process of both MLP and SVM algorithms, while preserving essential information about land characteristics.

2.4. Classification Models

The Multilayer Perceptron (MLP) is a type of artificial neural network (ANN) known for its high capability in capturing non-linear and complex relationships between features, particularly in spatial-

P-ISSN: 2723-3863 https://jutif.if.unsoed.ac.id E-ISSN: 2723-3871 DOI: https://doi.org/10.52436/1.jutif.2025.6.5.5179

Vol. 6, No. 5, October 2025, Page. 3153-3172

temporal data-based classification tasks [47]. In this study, the MLP was employed to classify changes in rice fields using spectral and textural features extracted from Sentinel-2 imagery [48]. The model architecture was designed to optimally map input characteristics into two target classes: change and no change. The MLP model was constructed with the following network structure [49]:

a. Input Layer

The input layer receives six primary extracted features: NDVI, NDWI, three GLCM-based texture features (contrast, homogeneity, entropy), and one principal component derived from PCA. The number of neurons in the input layer corresponds to the number of input features, resulting in 6 neurons.

b. Hidden Layers

The model comprises two hidden layers containing 64 and 32 neurons, respectively. This configuration was chosen to balance model complexity and prevent overfitting while enabling the network to capture non-linear patterns in the data. Each neuron employs the Rectified Linear Unit (ReLU) activation function, which is effective in deep networks due to its ability to mitigate the vanishing gradient problem and accelerate convergence.

c. Output Layer

The output layer consists of a single neuron with a sigmoid activation function, converting the output into a probabilistic value between 0 and 1. The sigmoid function is appropriate for binary classification problems, as it directly models the likelihood that a pixel or spatial unit belongs to the "land change" or "no change" class.

For the training process, the Adam (Adaptive Moment Estimation) optimization algorithm was utilized. Adam combines the strengths of the RMSProp and momentum algorithms and can adapt to gradient changes efficiently. It was selected for its stability and effectiveness in handling datasets with uneven distributions and features of varying scales [50].

The model was trained for 200 epochs with a batch size of 32, meaning the training data was divided into mini-batches of 32 samples per iteration. The number of epochs was determined based on preliminary testing of loss function convergence and validation performance stability. To prevent overfitting, an early stopping technique was applied based on the validation loss. If no improvement was observed over a number of consecutive epochs, the training process was halted early. The model was trained using 80% of the dataset with stratified k-fold cross-validation to ensure robust generalization.

The Support Vector Machine (SVM) is a widely used machine learning technique in remote sensing image classification due to its efficiency and accuracy in handling high-dimensional data [51]. Based on the principle of maximum margin, SVM aims to identify a separating hyperplane that maximizes the margin between classes, thereby reducing the risk of generalization error [52]. In this study, SVM was used as a comparative model to the MLP in classifying rice field changes based on features extracted from Sentinel-2 imagery. SVM was selected due to its robustness with limited training data and stability in datasets with good class separability.

Kernel Function

The SVM model was configured with a Radial Basis Function (RBF) kernel, a commonly used non-linear kernel that implicitly maps data into a higher-dimensional feature space. This enables the model to classify patterns that are not linearly separable in the original feature space, a frequent condition in spatial datasets with variable characteristics such as rice fields [53].

b. Parameter Tuning (Hyperparameter Optimization)

The two main SVM parameters, C and gamma, were optimized using a grid search approach, a systematic method of evaluating parameter combinations based on cross-validation performance. The regularization parameter C = 10 controls the trade-off between maximizing the margin and minimizing classification error. Higher C values tend to produce a model that fits the training data DOI: https://doi.org/10.52436/1.jutif.2025.6.5.5179

more tightly. The gamma parameter, set to 0.1, determines the influence of individual data points. This value was chosen to strike a balance between bias and variance, helping to avoid overfitting and ensure model generalizability.

Model Validation

E-ISSN: 2723-3871

The performance evaluation of the SVM model was conducted using a cross-validation scheme with k = 5, in which the training data was divided into five subsets (folds). The model was iteratively trained on four subsets and tested on the fifth. This technique was employed to measure model stability and prevent evaluation bias resulting from unrepresentative data partitioning. Model performance was then quantitatively compared with that of the MLP model using the same evaluation metrics: accuracy, precision, recall, F1-score, and the Kappa coefficient. This comparison enabled a comprehensive analysis of the advantages and limitations of each algorithm in classifying rice field changes within the study area.

2.5. Evaluation Metrics

The effectiveness of the classification models in detecting paddy field conversion was evaluated through two complementary approaches: quantitative assessment and spatial validation. Both Multilayer Perceptron (MLP) and Support Vector Machine (SVM) were examined to ensure a comprehensive evaluation of classification accuracy and robustness.

For the quantitative part, the evaluation relied on a confusion matrix framework, which consists of four fundamental components: True Positive (TP), representing correctly classified instances of paddy field conversion; False Positive (FP), denoting non-converted areas that were incorrectly labeled as converted; True Negative (TN), referring to correctly identified non-converted areas; and False Negative (FN), which captures actual conversions that the model failed to detect. Based on these values, several well-established metrics were employed. Accuracy represents the ratio of correctly classified samples to the total number of observations, though it may provide misleading results when class distributions are imbalanced. Precision measures the proportion of TP predictions among all positive predictions, which is essential to minimize FP occurrences. Recall evaluates the ability of the model to identify actual positive cases, making it particularly important in change detection where undetected conversions (FN) should be avoided. F1-score combines precision and recall into a single value using their harmonic mean, offering a balanced assessment when both metrics are equally critical.

In addition, the Receiver Operating Characteristic (ROC) curve was used to illustrate the tradeoff between sensitivity (TP rate) and 1-specificity (FP rate), while the Area Under the Curve (AUC) served as a global indicator of the model's discriminatory capability, with larger values indicating stronger performance.

To complement statistical evaluation, spatial validation was carried out by comparing classification outputs with a reference dataset (ground truth) generated from visual interpretation, field surveys, or trusted secondary sources. This procedure assessed how well the classification maps corresponded to actual conditions. By overlaying predicted maps with the reference, pixel-by-pixel agreement could be measured, enabling the detection of systematic errors such as overestimation or underestimation of converted areas. This step is particularly crucial in spatial planning and agricultural land monitoring, where positional accuracy is as important as statistical measures.

Evaluation metrics such as Accuracy, Precision, Recall, and F1 score were calculated using their standard formulas, as shown in Table 1. For ROC-AUC analysis, ROC curves were plotted across varying thresholds, and the AUC was obtained as a scalar summary of overall separability. Spatial validation was conducted through pixel-level overlay between classified maps and the reference dataset. All numerical metrics were calculated using Python's scikit-learn library, while spatial analysis and overlay operations were performed in QGIS 3.40.

E-ISSN: 2723-3871

https://jutif.if.unsoed.ac.id

DOI: https://doi.org/10.52436/1.jutif.2025.6.5.5179

Table 1. Evaluation Metrics

Measure	Formula
Precision	= <u>TP</u>
	-TP + FP
Recall	$=\frac{TP}{}$
	-TP + FN
F-measure	$= 2 * \frac{Recall * Precision}{}$
	$= 2 * {Recall + Precision}$
Accuracy	TP + TN
	$={TP+FP++FN+TN}$
Specificity	TN
•	$\equiv {TN + FP}$

3. RESULT

3.1. Data Collecting

The main dataset employed in this research comprises Sentinel-2 multispectral imagery from 2022, 2023, and 2024, covering the administrative area of Koto Tangah District (Figure 1) and summarized in Table 2. The imagery was obtained from two sources: Google Earth Engine (GEE) and the Copernicus Data Space Ecosystem, with the purpose of ensuring data availability within the required temporal range.

Table 2. Data Collecting

Year	Source	Sensor	Bands Used - Spatial Resolution	Cloud Coverage (%)	Format
2022	GEE dan Copernicus	MSI	B2, B3, B4, B8 = 10 m B11, B12 = 20m	< 30%	GeoTIFF
2023	GEE dan Copernicus	MSI	B2, B3, B4, B8 = 10 m B11, B12 = 20m	< 30%	GeoTIFF
2024	GEE dan Copernicus	MSI	B2, B3, B4, B8 = 10 m B11, B12 = 20m	< 30%	GeoTIFF

3.2. Data Preprocessing

Preprocessing was carried out by filtering the imagery within the defined Area of Interest (AOI) using the Google Collaboratory platform. The procedure included filtering by location and acquisition date, applying cloud-percentage thresholds, generating a median composite, and clipping to the study area. These steps ensured that the resulting datasets captured meaningful differences in imagery.

The process began with selecting images based on their spatial coverage and acquisition timeframe to guarantee relevance to the study period. Subsequently, filtering by cloud cover percentage was applied to minimize atmospheric disturbances and reduce cloud contamination, which can negatively impact classification accuracy. The retained images were then composited using the median

Vol. 6, No. 5, October 2025, Page. 3153-3172

P-ISSN: 2723-3863 E-ISSN: 2723-3871

method to suppress noise and provide more stable reflectance values across acquisition dates. This approach produced clearer satellite imagery for analysis, as illustrated in Figure 3 dan Figure 4.



Figure 3. (a) Raw Satellite Imagery (Before Filtering) 2022, (b) Satellite Image (After Filtering) 2022

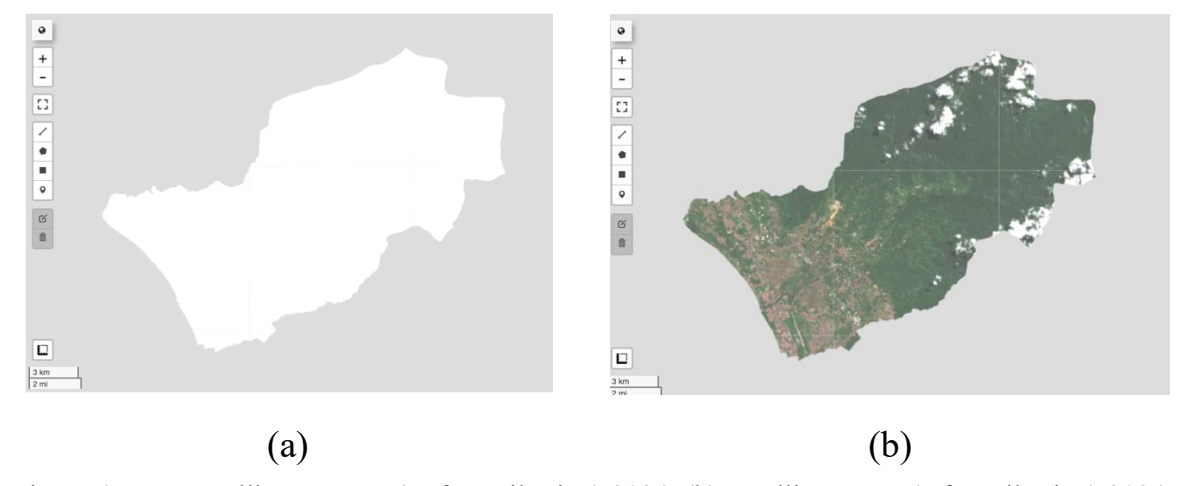


Figure 4. Raw Satellite Imagery (Before Filtering) 2024, (b) Satellite Image (After Filtering) 2024

Figures 3.a and 4.a illustrate satellite imagery that is still influenced by atmospheric disturbances and relatively high cloud coverage, especially in the central to northern regions of the study area. These conditions reduce the visual clarity of the imagery, making land cover interpretation more challenging. As a result, the contrast between vegetated and non-vegetated areas becomes less distinguishable, indicating the need for further image correction.

Meanwhile, Figures 3.b and 4.b present imagery that has undergone median compositing and the selection of scenes with lower cloud percentages. This preprocessing step produces a clearer representation of the study area, allowing better differentiation between vegetation (displayed in dark green), built-up areas and open land (displayed in reddish-brown), as well as the remaining cloud cover. The contrast between these two sets of imagery highlights the critical role of preprocessing techniques particularly cloud filtering and image compositing in obtaining more reliable spatial information and supporting subsequent analytical processes.

E-ISSN: 2723-3871

DOI: https://doi.org/10.52436/1.jutif.2025.6.5.5179

3.3. Spectral and Textural Feature Extraction Results

Figure 5 presents the histograms of Sentinel-2 bands (B2, B3, B4, and B8), illustrating the differences in digital number (DN) value distributions between raw and preprocessed imagery. In the raw image, DN values are more broadly spread, with the highest frequency appearing around the midrange. In contrast, the preprocessed image shows a more concentrated distribution, predominantly within the lower DN range. These changes indicate that the radiometric and atmospheric correction processes have successfully adjusted the surface reflectance values to better represent actual conditions in the field. For example, in Band 8 (NIR), a shift in the distribution toward higher values is observed, indicating improved vegetation information. Meanwhile, in the visible bands (B2, B3, and B4), the shift in the distribution toward lower DN values indicates a reduction in atmospheric effects and improved contrast between objects.

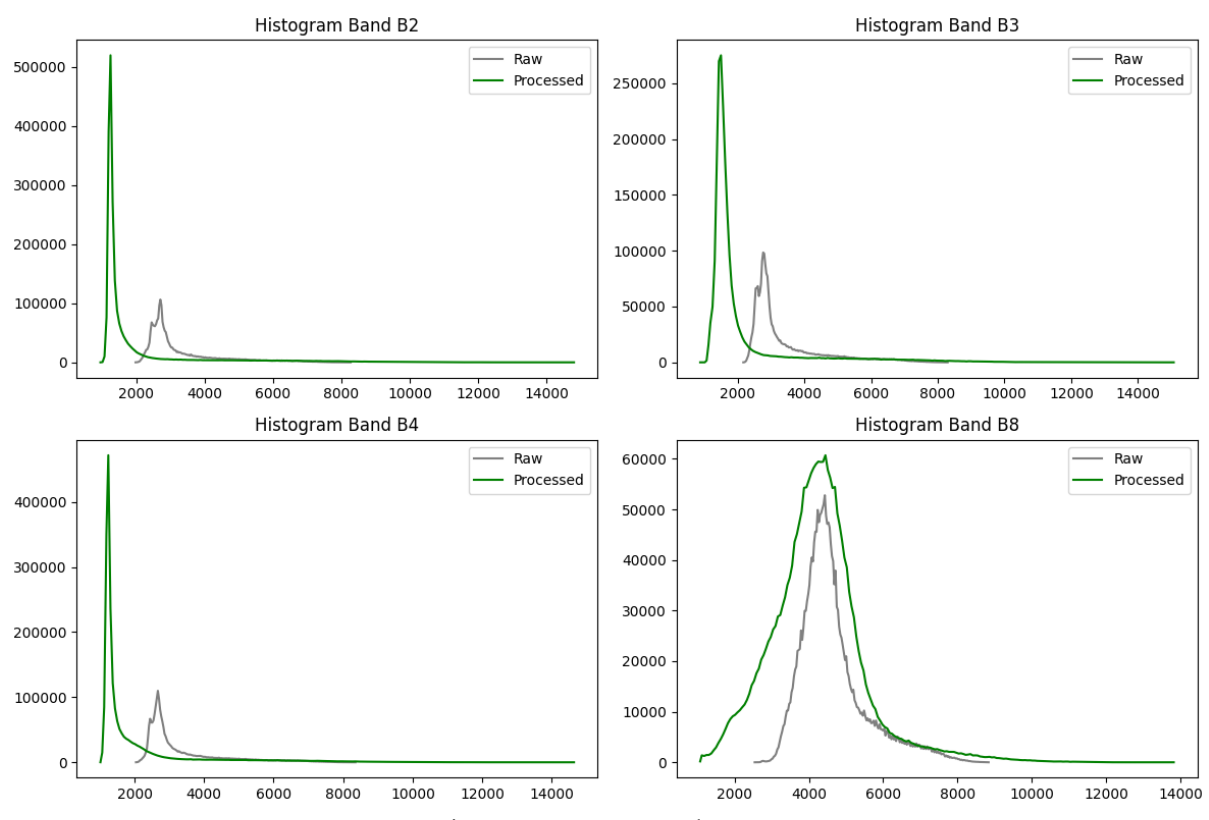


Figure 5. Preprocessed Image

Figure 6 presents a histogram of NDVI (Normalized Difference Vegetation Index) values in Padang City for 2022, derived from post-processed Sentinel-2 imagery. The histogram illustrates the distribution of vegetation values in terms of pixel frequency across NDVI value ranges. The horizontal axis (X-axis) represents NDVI values, which theoretically range from -1 to +1; however, the values in this histogram fall between -0.2 and +0.8. NDVI values below zero generally correspond to non-vegetated features such as water bodies, built-up areas (e.g., buildings and roads), or bare land. In contrast, values above zero indicate vegetated areas, with higher values signifying healthier and denser vegetation.

The vertical axis (Y-axis) shows the number of pixels within each NDVI range, reflecting the relative spatial extent of various land cover types based on vegetation density. Principal Component Analysis (PCA) was successfully used to reduce feature dimensionality without significantly compromising important information.

E-ISSN: 2723-3871

DOI: https://doi.org/10.52436/1.jutif.2025.6.5.5179

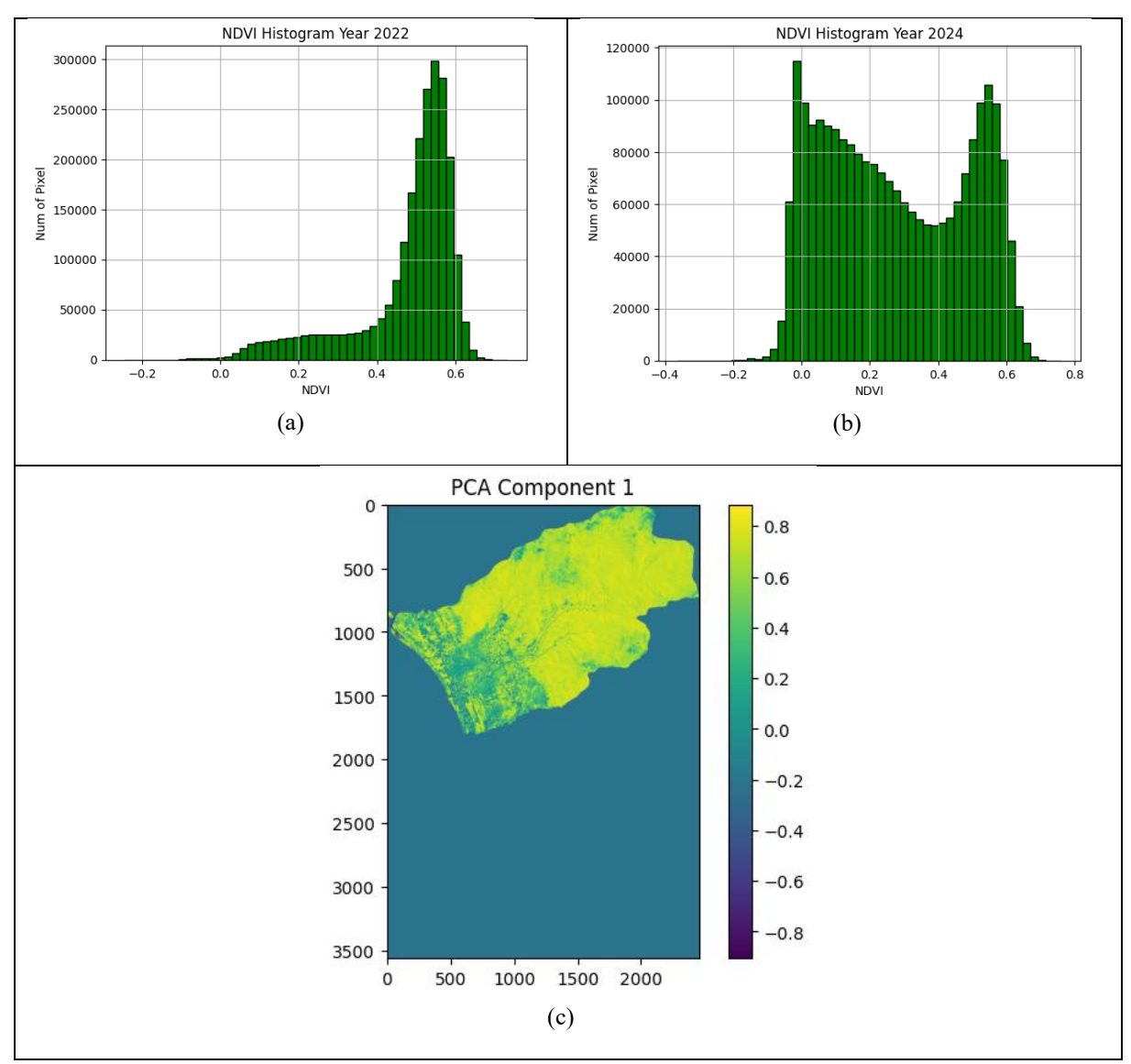


Figure 6. Feature Extraction Results
(a) NDVI 2022, (b) NDVI 2024, (c) Composite Band PCA

Based on the histogram of Figure 6, the majority of NDVI values are concentrated between 0.5 and 0.6, with the mode around 0.55. This suggests that, during the observation year, most areas in Padang City exhibited moderate to high vegetation density, indicative of active rice fields, shrublands, or other well-established vegetation. Conversely, NDVI values below 0.2 account for only a small number of pixels, indicating that areas with very little or no vegetation (e.g., dense settlements, open fields, or water bodies) occupy a relatively smaller area compared to vegetated regions. Furthermore, the number of pixels with NDVI values above 0.6 decreases drastically, suggesting that only a limited area contains very dense vegetation, such as primary forests or rice fields at their peak growing season. Overall, this distribution pattern indicates that Padang City in 2022 remained dominated by medium to high vegetation density, highlighting the significance of sustainable green spaces and productive agriculture amid increasing urbanization pressures.

The NDVI distribution histogram for 2024 provides a comprehensive overview of vegetation conditions in Padang City based on Sentinel-2 remote sensing imagery. NDVI values are shown on the

E-ISSN: 2723-3871

Vol. 6, No. 5, October 2025, Page. 3153-3172 https://jutif.if.unsoed.ac.id

DOI: https://doi.org/10.52436/1.jutif.2025.6.5.5179

horizontal (X) axis, ranging from -0.35 to +0.75, while the vertical (Y) axis represents the number of pixels in each NDVI class, reflecting the relative extent of each land cover category. An NDVI value below 0 generally corresponds to non-vegetative areas such as water bodies, bare soil, or artificial surfaces like buildings. Values between 0.1 and 0.4 indicate sparse vegetation or early-stage plant growth, whereas values above 0.5 to 0.75 correspond to dense vegetation, such as actively growing rice fields.

The 2024 histogram displays an interesting bimodal pattern, with two prominent distribution peaks. The first peak appears around NDVI values of 0.0–0.1, while the second lies in the range of 0.55– 0.6. The emergence of the first peak, more prominent than in 2022 indicates an increase in areas with very low or no vegetation. This change may be attributed to land use conversion, fallow rice fields between planting seasons, or expansion of water bodies. Meanwhile, the second, relatively stable peak at NDVI > 0.5 suggests that areas with dense vegetation such as active rice fields, home gardens, or unconverted natural vegetation remain present.

This distribution pattern indicates that, while pockets of healthy vegetation persist in Padang City, there was a significant expansion of non-vegetative areas in 2024. This finding underscores the urgency of protecting productive agricultural land and promoting data-driven spatial planning policies to prevent further degradation of vegetation cover.

A comparison of the NDVI distributions between 2022 and 2024 reveals notable changes in vegetative land cover characteristics in Padang City. In 2022, the NDVI distribution was dominated by a single peak in the 0.55-0.6 range, reflecting the dominance of areas with dense vegetation, such as active and healthy rice fields. However, by 2024, the distribution had shifted to a bimodal pattern, with a new peak emerging around NDVI values of 0.0-0.1, indicating increased areas with little or no vegetation. This shift suggests land cover degradation or conversion of rice fields to non-agricultural uses. Although the high NDVI peak (>0.5) remains, the sharp increase in low NDVI values signals growing pressure on productive agricultural land and highlights the need for continuous spatial monitoring to support sustainable land use and conservation policies.

3.4. Results of Rice Field Change Classification Using the MLP Method

The Multilayer Perceptron (MLP) model implemented in this study achieved an overall accuracy of 71% in classifying paddy and non-paddy fields across a total of 7,961 sample pixels. Further evaluation metrics revealed a precision of 0.92 and a recall of 0.53 for the paddy field class (label 0), resulting in an F1-score of 0.68. These values indicate that the model is highly effective at correctly identifying true paddy field pixels (high precision), but less effective at detecting all relevant paddy field areas (low recall).

In contrast, for the non-paddy field class (label 1), the MLP yielded a very high recall of 0.94, demonstrating the model's strong ability to identify most non-paddy field pixels. Although its precision was lower at 0.62, the resulting F1-score of 0.75 indicates a more balanced performance for the nonpaddy class compared to the paddy class.

The confusion matrix supports these findings with 2.3740 paddy field pixels were correctly classified, however 2.0670 paddy field pixels were misclassified as non-paddy. Meanwhile, 3.3170 nonpaddy pixels were correctly classified. Only 203 non-paddy pixels were incorrectly classified as paddy fields.

Overall, the model tends to be more sensitive to the non-rice field class and less capable of comprehensively detecting the rice field class, as indicated by the imbalanced recall values between the two classes. This condition may be attributed to an unbalanced distribution of training data, high spectral variability within rice fields, or spatial complexity that is not fully captured by the MLP architecture used.

P-ISSN: 2723-3863

Vol. 6, No. 5, October 2025, Page. 3153-3172 https://jutif.if.unsoed.ac.id DOI: https://doi.org/10.52436/1.jutif.2025.6.5.5179

For agricultural land monitoring applications and rice field protection policymaking, low recall in the rice field class is a significant concern. This can result in underestimating the actual extent of existing rice fields, leading to misinterpretations in spatial planning. Therefore, efforts to enhance model performance, such as incorporating more diverse training data, integrating additional spatial features, or employing a hybrid classification approach, should be considered in future work.

Results of Rice Field Change Classification Using the SVM Method

Table 3 presents the results of applying the Support Vector Machine (SVM) algorithm to classify rice fields and non-rice fields using NDVI, NDWI, and two principal components derived from Principal Component Analysis (PCA). Based on the evaluation results, the SVM model achieved an overall accuracy of 71% across 7,961 test pixels.

For the rice field class (label 0), the model achieved a precision of 0.91, indicating that most predicted rice field pixels were correctly classified. However, the recall was only 0.54, meaning the SVM failed to detect nearly half of the actual rice paddy areas. The resulting F1-score of 0.68 reflects the imbalance between precision and recall for this class.

In contrast, for the non-rice paddy class (label 1), the SVM demonstrated stronger recall performance at 0.94, indicating excellent detection of non-rice paddy areas. However, its precision was lower at 0.62, suggesting a notable number of misclassifications where rice paddy pixels were incorrectly labeled as non-rice paddy. The F1-score for this class was 0.74, indicating relatively more stable performance than that observed for the rice paddy class.

These results suggest that the SVM model is more sensitive to the non-rice paddy class and tends to overpredict this label. While SVM is capable of handling high-dimensional data and defining clear class boundaries, its limitations in modeling complex and non-linear patterns likely contribute to the low recall observed for the rice paddy class. In the context of rice field classification, this low recall poses a significant challenge, as it can lead to underrepresentation of rice fields in spatial data, thereby affecting the accuracy of information used in policymaking for sustainable agricultural land protection.

Table 3. Comparison of SVM and MLP Performance

Metrik	SVM	MLP
Accuracy	0.71	0.82
Precision (paddy field)	0.91 (label 0)	0.92 (label 0)
Recall (paddy field)	0.54 (label 0)	0.53 (label 0)
F1-score (paddy field)	0.68	0.68
Precision (Non-paddy field)	0.62 (label 1)	0.62 (label 1)
Recall (Non-paddy field)	0.94	0.94
F1-score (Non-paddy field)	0.74	0.75

Overall, although the SVM's overall accuracy is comparable to that of the MLP model, classwise performance reveals that MLP offers a more balanced classification, particularly in identifying complex, non-linear characteristics within the rice field class. These findings underscore the potential advantages of neural network-based approaches like MLP for future agricultural land monitoring systems.

Quantitative Evaluation of Model Performance 3.6.

This study compares the performance of two machine learning algorithms, Multilayer Perceptron (MLP) and Support Vector Machine (SVM) in classifying rice field and non-rice field changes based on NDVI and NDWI features, along with two principal components derived from Principal Component

https://jutif.if.unsoed.ac.id

Vol. 6, No. 5, October 2025, Page. 3153-3172

DOI: https://doi.org/10.52436/1.jutif.2025.6.5.5179

Analysis (PCA). The evaluation employed common metrics for binary classification tasks: accuracy, precision, recall, and F1-score.

The classification results using the MLP algorithm demonstrated relatively balanced performance, with an overall accuracy of 71%. For the rice field class (label 0), the MLP achieved a precision of 0.92 and a recall of 0.53, indicating that the model was highly precise in identifying rice fields but exhibited limitations in comprehensively capturing all rice field areas. For the non-rice field class (label 1), the model recorded a precision of 0.62 and a recall of 0.94, resulting in F1-scores of 0.68 and 0.75, respectively. The macro-average F1-score of 0.71 suggests that the MLP model effectively balances accuracy and completeness across both classes.

Similarly, the SVM algorithm exhibited a comparable overall accuracy of 71%, but with a more imbalanced performance. For the non-rice field class, the SVM achieved a high recall of 0.94 but only a 0.62 precision, resulting in an F1-score of 0.74. For the rice field class, the precision was 0.91 while the recall was 0.54, yielding an F1-score of 0.68. Although the overall accuracy and F1-scores were similar to those of the MLP, the SVM tended to favor the non-rice field class and was less capable of identifying the more complex spatial and non-linear variations within the rice field class.

Visually, confusion matrix analysis showed that the MLP resulted in slightly fewer misclassifications in the non-rice field class compared to the SVM, although both models struggled to detect the full extent of rice fields (recall < 0.6). The MLP's ability to model non-linear patterns and spatial dependencies between pixels contributed to its superior performance in capturing the dynamics of rice field vegetation, particularly when using a combination of vegetation indices and PCA-derived features.

Based on the evaluation results, it can be concluded that the MLP is more effective in maintaining balanced classification performance across classes, whereas the SVM performs better in identifying the majority class (non-rice fields), albeit at the expense of recall in the minority class (rice fields). These findings suggest that for satellite imagery-based agricultural monitoring in areas with high spatial complexity, deep learning approaches such as MLP may offer greater adaptability and accuracy than conventional margin-based methods like SVM.

3.7. **Spatial Analysis and Validation of Results**

The classification outcomes generated by the Multilayer Perceptron (MLP) and Support Vector Machine (SVM) algorithms were visualized as spatial maps illustrating the distribution of rice and nonrice field classes across the study area. Spatially, the MLP model produced smoother delineations of rice field boundaries and better conformed to natural spatial contours, while the SVM yielded sharper segmentations but introduced noise in heterogeneous regions.

Spatial validation was conducted by comparing the classification outputs with reference data derived from polygon labels of rice and non-rice field areas. MLP achieved an accuracy of 82%, outperforming SVM, which reached 71%. However, the MLP recorded a precision of 0.92 and a recall of 0.53 for the rice field class, and 0.62 and 0.94 for the non-rice field class, resulting in an F1-score of 0.75 for the non-rice class. In contrast, the SVM produced a slightly lower F1-score of 0.74 and lower precision for the non-rice field class compared to the MLP. This indicates that the MLP model was more effective at detecting non-rice field areas while minimizing false positives in rice field classification.

4. **DISCUSSIONS**

Algorithm Performance Analysis in Spatial and Statistical Contexts

The Multilayer Perceptron (MLP) algorithm achieved a classification accuracy of 82%, whereas the Support Vector Machine (SVM) obtained 71% overall accuracy. Notable differences emerged in class-specific performance metrics. The MLP consistently detected non-rice field pixels with a recall of

https://jutif.if.unsoed.ac.id E-ISSN: 2723-3871 DOI: https://doi.org/10.52436/1.jutif.2025.6.5.5179

Vol. 6, No. 5, October 2025, Page. 3153-3172

0.94. For the rice field class, it reached a precision of 0.92 but only a recall of 0.53, comparable to the SVM outcomes. This trend suggests that the MLP model is more effective at recognizing the majority class (non-rice fields) than SVM, a common issue when dealing with imbalanced datasets.

The superior performance of MLP can be attributed to its ability to model non-linear relationships among features such as NDVI, NDWI, and PCA components, thereby improving classification accuracy in areas with complex vegetation structures. This demonstrates the strength of neural network-based approaches in capturing subtle spatial variations, positioning MLP as a promising technique for highresolution agricultural land classification. Conversely, although SVM is generally robust to overfitting and performs well with limited datasets, it often produces noisier spatial results. This is evident in its classification maps, which contain numerous random patches within homogeneous areas, reflecting its limitations in capturing the spatial context between pixels.

Previous studies provide additional perspective. Huo found that SVM outperformed MLP in classifying Near-Infrared (NIR) data, which involved linear data with a single band[54]. Similarly, Marji's work on linear datasets also confirmed SVM's advantage [55]. However, in this study, MLP surpassed SVM in handling non-linear data. Consistent with Jamali's findings, MLP achieved higher accuracy in land change classification, which was attributed to the complexity of composite bands [56]. Fattah also reported that MLP outperformed SVM in land change classification, emphasizing its strength in integrating multiple spectral bands for land-cover analysis [57].

Spatial Validation and Relevance to Field Conditions

Spatial validation further supports these results, showing that the MLP model generates more detailed and realistic classifications that align with natural patterns in agricultural landscapes. The model delineates rice field boundaries more precisely, matching reference maps derived from visual interpretation and field surveys. By contrast, SVM produces less spatially accurate segmentations, often oversimplifying complex structures into unrealistic, linear boundaries.

This finding is particularly significant in land mapping and spatial planning, where accuracy is critical for determining land status. Misclassification of active rice fields may lead to substantial policy implications, especially when designating agricultural protection zones.

4.3. **Implications for Land Monitoring and Policy**

The findings of this study provide practical implications for policymakers, particularly regarding land conversion monitoring and spatially optimized land-use planning. Integrating the MLP classification model into spatial platforms such as WebGIS could substantially enhance automated and interactive land monitoring systems, especially in regions under high development pressure. A validated MLP model can also function as an early warning tool to detect initial signs of rice field conversion. Moreover, by incorporating temporal analysis, the system could reveal annual patterns of land change and inform the development of evidence-based spatial policies.

Limitations and Directions for Further Research

Several limitations should be acknowledged. First, the class imbalance between paddy and nonpaddy fields reduces recall performance for the paddy class. Second, relying solely on NDVI, NDWI, and PCA-based features cannot fully capture spatial complexity. Although MLP outperformed SVM overall, significant misclassification was still observed in transitional zones. Future studies should consider expanding the amount and spatial diversity of training data, as well as integrating contextual features, such as proximity to roads or digital elevation model (DEM) data to improve model performance in distinguishing paddy from non-paddy areas.

Beyond its spatial and agricultural relevance, this research advances the field of computer science by demonstrating the capability of Multilayer Perceptron (MLP) to support scalable and automated land

https://jutif.if.unsoed.ac.id

DOI: https://doi.org/10.52436/1.jutif.2025.6.5.5179

Vol. 6, No. 5, October 2025, Page. 3153-3172

monitoring systems. The superior performance of MLP in handling non-linear spectral and textural features highlights its potential for real-time integration into WebGIS platforms. Such integration would enable continuous monitoring of rice field dynamics, facilitating automated alerts on land conversion and providing decision-makers with up-to-date spatial intelligence. From an informatics perspective, this study strengthens the role of neural network-based models in spatio-temporal data analysis, bridging the gap between remote sensing applications and intelligent information systems. Ultimately, the findings contribute to the development of machine learning pipelines that can be generalized for broader environmental monitoring tasks, including urban expansion, deforestation, and crop yield prediction.

5. **CONCLUSION**

E-ISSN: 2723-3871

This study examined rice field changes in Koto Tangah District, Padang City, using Sentinel-2 satellite imagery from 2022-2024. Image processing involved the use of NDVI and NDWI vegetation indices, along with texture analysis and Principal Component Analysis (PCA). The results indicate a decline in dense vegetation areas, particularly in active rice fields, as shown by a reduction in the number of pixels with NDVI values greater than 0.5 in 2024. Furthermore, the 2024 NDVI histogram revealed a new peak in the lower value range (around 0.0-0.1), suggesting an increase in non-vegetated areas such as idle land, converted land, or waterlogged zones.

To identify spatial changes, two classification methods were employed: Multilayer Perceptron (MLP) and Support Vector Machine (SVM). For the non-rice field class, MLP achieved a precision of 0.62, a recall of 0.94, and an F1-score of 0.75. SVM produced comparable outcomes, though with slightly lower precision. In terms of overall performance, MLP attained an accuracy of 82%, surpassing SVM, which achieved 71%. These results highlight the strength of MLP in capturing complex spatial patterns, as its architecture effectively models non-linear relationships among features.

In conclusion, the MLP-based classification approach is more effective for mapping rice field changes in complex spatial environments. The findings not only support agricultural land protection and sustainable urban development but also advance computer science by reinforcing the role of machine learning in spatio-temporal data analysis and demonstrating the strength of non-linear models in satellite image classification.

For future research, several improvements can be pursued. First, the integration of additional features such as digital elevation models (DEM), proximity to infrastructure, or socio-economic data could enhance classification robustness. Second, expanding the diversity and volume of training data would help mitigate class imbalance and improve generalization. Finally, exploring deep learning architectures—such as Convolutional Neural Networks (CNN), Recurrent Neural Networks (RNN), or hybrid models—may further increase accuracy and scalability, paving the way toward fully automated, real-time land monitoring systems.

REFERENCES

- V. Mutiara, R. Febriamansyah, R. Hariance, and A. S. Utami, "Farmers' resilience towards land [1] use change case study in Padang City, West Sumatra, Indonesia)," IOP Conf. Ser.: Earth Environ. Sci., vol. 583, no. 1, p. 012014, Oct. 2020, doi: 10.1088/1755-1315/583/1/012014
- BPS-Statistics Indonesia West Sumatera, Paddy and Rice Production by Regency/City in West [2] Sumatra Province. [Online]. Available: https://sumbar.bps.go.id/en/statisticstable/3/ZDNaak0yODBUVTlGYW5sa2REUkVUVVY1YVZkbmR6MDkjMyMxMzAw/paddy -and-rice-production-sup-1--sup--by-regency-municipality-in-sumatera-baratprovince.html?year=2022. (Accessed: Sept. 01, 2025)
- J. Oakleaf et al., "Mapping global land conversion pressure to support conservation planning," Sci Data, vol. 11, no. 1, July 2024, doi: 10.1038/s41597-024-03639-9

Vol. 6, No. 5, October 2025, Page. 3153-3172 P-ISSN: 2723-3863 https://jutif.if.unsoed.ac.id E-ISSN: 2723-3871 DOI: https://doi.org/10.52436/1.jutif.2025.6.5.5179

[4] J. C. Onwe, M. G. Ojide, M. Subhan, and D. Forgenie, "Food security in Nigeria amidst globalization, economic expansion, and population growth: A wavelet coherence and QARDL analysis," Journal of Agriculture and Food Research, vol. 18, p. 101413, Dec. 2024, doi: 10.1016/j.jafr.2024.101413

- "Urbanisation, Paddy Field Conversion and its Impact on Rice Production in Indonesia: A [5] Synthesis of Panel Data 2015–2019," in Advances in Intelligent Systems Research, Dordrecht: Atlantis Press International BV, 2024, pp. 249–262. doi: 10.2991/978-94-6463-445-7 28
- [6] S. Zhang et al., "Monitoring the Spatio-Temporal Changes of Non-Cultivated Land via Long-Time Series Remote Sensing Images in Xinghua," *IEEE Access*, vol. 10, pp. 84518–84534, 2022, doi: 10.1109/ACCESS.2022.3197650
- [7] Z. Lu, W. Li, and S. Zhou, "Constructing a resilient ecological network by considering source stability in the largest Chinese urban agglomeration," Journal of Environmental Management, vol. 328, p. 116989, Feb. 2023, doi: 10.1016/j.jenvman.2022.116989
- C. Zhao et al., "Evaluating ecological conservation effectiveness of security patterns under [8] multiple scenarios: A case study of Hubei Province," Ecological Indicators, vol. 166, p. 112528, Sept. 2024, doi: 10.1016/j.ecolind.2024.112528
- W. Hu, K. Xiong, M. Zhang, and L. You, "Land use change impact on the ecosystem service [9] value in karst desertification control zone," npj Heritage Science, vol. 13, no. 1, June 2025, doi: 10.1038/s40494-025-01860-2
- "UU No. 41 Tahun 2009," Database Peraturan | JDIH BPK. [Online]. Available: http://peraturan.bpk.go.id/Details/38786/uu-no-41-tahun-2009. (Accessed: July 13, 2025)
- [11] K. Kirby, S. Ferguson, C. D. Rennie, J. Cousineau, and I. Nistor, "Identification of the best method for detecting surface water in Sentinel-2 multispectral satellite imagery," Remote Sensing Applications: Society and Environment, vol. 36, p. 101367, Nov. 2024. 10.1016/j.rsase.2024.101367
- [12] A. Ansari et al., "Evaluating the effect of climate change on rice production in Indonesia using multimodelling approach," Heliyon, vol. 9, no. 9, p. e19639, Sept. 2023, doi: 10.1016/j.heliyon.2023.e19639
- [13] S. Wang, W. Han, X. Huang, X. Zhang, L. Wang, and J. Li, "Trustworthy remote sensing interpretation: Concepts, technologies, and applications," ISPRS Journal of Photogrammetry and Remote Sensing, vol. 209, pp. 150-172, Mar. 2024, doi: 10.1016/j.isprsjprs.2024.02.003
- [14] M. Aghaabbasi and S. Chalermpong, "Machine learning techniques for evaluating the nonlinear link between built-environment characteristics and travel behaviors: A systematic review," Travel Behaviour and Society, vol. 33, p. 100640, Oct. 2023, doi: 10.1016/j.tbs.2023.100640
- Y. Yang, T. Nikolaidis, S. Jafari, and P. Pilidis, "Gas turbine engine transient performance and heat transfer effect modelling: A comprehensive review, research challenges, and exploring the future," Applied Thermal Engineering, vol. 236, p. 121523, Jan. 2024, 10.1016/j.applthermaleng.2023.121523
- [16] A. A. Khan, O. Chaudhari, and R. Chandra, "A review of ensemble learning and data augmentation models for class imbalanced problems: Combination, implementation and evaluation," Expert Systems with Applications, vol. 244, p. 122778, June 2024, doi: 10.1016/j.eswa.2023.122778
- [17] M. A. K. Raiaan et al., "A systematic review of hyperparameter optimization techniques in Convolutional Neural Networks," *Decision Analytics Journal*, vol. 11, p. 100470, June 2024, doi: 10.1016/j.dajour.2024.100470
- [18] Z. Quan and L. Pu, "An improved accurate classification method for online education resources based on support vector machine (SVM): Algorithm and experiment," Educ Inf Technol, vol. 28, no. 7, pp. 8097–8111, July 2023, doi: 10.1007/s10639-022-11514-6
- H. Li, L. Jiang, E. D. Ganaa, P. Li, and X.-J. Shen, "Robust feature enhanced deep kernel support vector machine via low rank representation and clustering," Expert Systems with Applications, vol. 271, p. 126612, May 2025, doi: 10.1016/j.eswa.2025.126612
- R. Guido, S. Ferrisi, D. Lofaro, and D. Conforti, "An Overview on the Advancements of Support Vector Machine Models in Healthcare Applications: A Review," Information, vol. 15, no. 4, p. 235, Apr. 2024, doi: 10.3390/info15040235

Vol. 6, No. 5, October 2025, Page. 3153-3172 P-ISSN: 2723-3863 https://jutif.if.unsoed.ac.id E-ISSN: 2723-3871 DOI: https://doi.org/10.52436/1.jutif.2025.6.5.5179

[21] J. S. Pimentel, R. Ospina, and A. Ara, "A novel fusion Support Vector Machine integrating weak and sphere models for classification challenges with massive data," Decision Analytics Journal, vol. 11, p. 100457, June 2024, doi: 10.1016/j.dajour.2024.100457

- J. Gu and R. G. Congalton, "Assessing the Impact of Mixed Pixel Proportion Training Data on SVM-Based Remote Sensing Classification: A Simulated Study," *Remote Sensing*, vol. 17, no. 7, p. 1274, Apr. 2025, doi: 10.3390/rs17071274
- [23] J. Nyengere et al., "Forest cover restoration analysis using remote sensing and machine learning in central Malawi," Trees, Forests and People, vol. 20, p. 100873, June 2025, doi: 10.1016/j.tfp.2025.100873
- [24] R. Franco, M. C. Torres-Madronero, M. Casamitjana, and T. Rondon, "Spatial-spectral feature extraction using multispectral linear unmixing for land use land cover change detection," Journal 105722, Oct. 2025, of South American Earth Sciences, vol. 165, p. 10.1016/j.jsames.2025.105722
- [25] Z. Zhu, S. Qiu, and S. Ye, "Remote sensing of land change: A multifaceted perspective," *Remote* Sensing of Environment, vol. 282, p. 113266, Dec. 2022, doi: 10.1016/j.rse.2022.113266
- [26] T. Wang et al., "An adaptive atmospheric correction algorithm for the effective adjacency effect correction of submeter-scale spatial resolution optical satellite images: Application to a WorldView-3 panchromatic image," Remote Sensing of Environment, vol. 259, p. 112412, June 2021, doi: 10.1016/j.rse.2021.112412
- [27] K. E. Lewińska, S. Ernst, D. Frantz, U. Leser, and P. Hostert, "Global overview of usable Landsat and Sentinel-2 data for 1982-2023," Data in Brief, vol. 57, p. 111054, Dec. 2024, doi: 10.1016/j.dib.2024.111054
- [28] C. Valdivieso-Ros, F. Alonso-Sarria, and F. Gomariz-Castillo, "Effect of Different Atmospheric Correction Algorithms on Sentinel-2 Imagery Classification Accuracy in a Semiarid Mediterranean Area," Remote Sensing, vol. 13, no. 9, p. 1770, May 2021, doi: 10.3390/rs13091770
- [29] L. A. Brown et al., "GROUNDED EO: Data-driven Sentinel-2 LAI and FAPAR retrieval using Gaussian processes trained with extensive fiducial reference measurements," Remote Sensing of Environment, vol. 326, p. 114797, Aug. 2025, doi: 10.1016/j.rse.2025.114797
- [30] J. Wang et al., "Automatic cloud and cloud shadow detection in tropical areas for PlanetScope satellite images," Remote Sensing of Environment, vol. 264, p. 112604, Oct. 2021, doi: 10.1016/j.rse.2021.112604
- [31] N. Wright, J. M. A. Duncan, J. N. Callow, S. E. Thompson, and R. J. George, "CloudS2Mask: A novel deep learning approach for improved cloud and cloud shadow masking in Sentinel-2 imagery," Remote Sensing of Environment, vol. 306, p. 114122, May 2024, doi: 10.1016/j.rse.2024.114122
- "Clouds and Image Compositing," in Cloud-Based Remote Sensing with Google Earth Engine, [32] Cham: Springer International Publishing, 2024, pp. 279–302. doi: 10.1007/978-3-031-26588-
- [33] P. A. Palanisamy, J. Zawadzka, K. Jain, S. Bonafoni, and A. Tiwari, "Assessing diurnal land surface temperature variations across landcover and local climate zones: Implications for urban planning and mitigation strategies on socio-economic factors," Sustainable Cities and Society, vol. 116, p. 105880, Dec. 2024, doi: 10.1016/j.scs.2024.105880
- [34] N. Quintero, O. Viedma, S. Veraverbeke, and J. M. Moreno, "Optimising fire severity mapping using pixel-based image compositing," Remote Sensing of Environment, vol. 321, p. 114687, May 2025, doi: 10.1016/j.rse.2025.114687
- [35] E. Barca, M. C. Caputo, and R. Masciale, "Building the optimal hybrid spatial Data-Driven Model: Balancing accuracy and complexity," International Journal of Applied Earth Observation and Geoinformation, vol. 139, p. 104478, May 2025, doi: 10.1016/j.jag.2025.104478
- T. K, R. Kumar, S. Ramadass, and S. Narayanan, "Satellite Remote Sensing Analysis Using Effective Feature Extraction Classification Using Deep Learning Technique." Springer Science and Business Media LLC, July 22, 2024. doi: 10.21203/rs.3.rs-4634861/v1
- [37] S. Amani and H. Shafizadeh-Moghadam, "A review of machine learning models and influential factors for estimating evapotranspiration using remote sensing and ground-based data,"

Vol. 6, No. 5, October 2025, Page. 3153-3172 P-ISSN: 2723-3863 https://jutif.if.unsoed.ac.id E-ISSN: 2723-3871 DOI: https://doi.org/10.52436/1.jutif.2025.6.5.5179

Water vol. 284, 108324, Agricultural Management, p. June 2023, doi: 10.1016/j.agwat.2023.108324

- [38] Q. Zhao and Y. Qu, "The Retrieval of Ground NDVI (Normalized Difference Vegetation Index) Data Consistent with Remote-Sensing Observations," Remote Sensing, vol. 16, no. 7, p. 1212, Mar. 2024, doi: 10.3390/rs16071212
- [39] Gessesse , Agenagnew A., "Temporal relationships between time series CHIRPS-rainfall estimation and eMODIS-NDVI satellite images in Amhara Region, Ethiopia," in Extreme Hydrology and Climate Variability, Elsevier, 2019, pp. 81–92. doi: 10.1016/b978-0-12-815998-
- T. R. Tenreiro, M. García-Vila, J. A. Gómez, J. A. Jiménez-Berni, and E. Fereres, "Using NDVI for the assessment of canopy cover in agricultural crops within modelling research," Computers Electronics Agriculture, vol. 182, p. 106038, 10.1016/j.compag.2021.106038
- [41] S. Samsuddin Sah, K. N. Abdul Maulud, S. Sharil, O. A. Karim, and B. Pradhan, "Monitoring of three stages of paddy growth using multispectral vegetation index derived from UAV images," The Egyptian Journal of Remote Sensing and Space Sciences, vol. 26, no. 4, pp. 989–998, Dec. 2023, doi: 10.1016/j.ejrs.2023.11.005
- [42] P. P. Patil, M. P. Jagtap, N. Khatri, H. Madan, A. A. Vadduri, and T. Patodia, "Exploration and advancement of NDDI leveraging NDVI and NDWI in Indian semi-arid regions: A remote sensing-based study," Case Studies in Chemical and Environmental Engineering, vol. 9, p. 100573, June 2024, doi: 10.1016/j.cscee.2023.100573
- [43] J. Tian, Y. Tian, Y. Cao, W. Wan, and K. Liu, "Research on Rice Fields Extraction by NDVI Difference Method Based on Sentinel Data," Sensors, vol. 23, no. 13, p. 5876, June 2023, doi: 10.3390/s23135876
- [44] N. Iqbal, R. Mumtaz, U. Shafi, and S. M. H. Zaidi, "Gray level co-occurrence matrix (GLCM) texture based crop classification using low altitude remote sensing platforms," PeerJ Computer Science, vol. 7, p. e536, May 2021, doi: 10.7717/peerj-cs.536
- [45] P. Mohammadpour, D. X. Viegas, A. Pereira, and E. Chuvieco, "Multitemporal Sentinel and GEDI data integration for overstory and understory fuel type classification," International Journal of Applied Earth Observation and Geoinformation, vol. 139, p. 104455, May 2025, doi: 10.1016/j.jag.2025.104455
- [46] N. A. Syam, N. Arifin, W. Firgiawan, and M. F. Rasvid, "Comparison of SVM and Gradient Boosting with PCA for Website Phising Detection," Jurnal Teknik Informatika (Jutif), vol. 6, no. 2, pp. 691–708, Apr. 2025, doi: 10.52436/1.jutif.2025.6.2.4344
- A. Dikshit, B. Pradhan, and M. Santosh, "Artificial neural networks in drought prediction in the 21st century-A scientometric analysis," Applied Soft Computing, vol. 114, p. 108080, Jan. 2022, doi: 10.1016/j.asoc.2021.108080
- [48] T. Qu et al., "A fine crop classification model based on multitemporal Sentinel-2 images," International Journal of Applied Earth Observation and Geoinformation, vol. 134, p. 104172, Nov. 2024, doi: 10.1016/j.jag.2024.104172
- [49] K. Y. Chan et al., "Deep neural networks in the cloud: Review, applications, challenges and *Neurocomputing*, vol. 545, p. 126327, Aug. 2023, directions," 10.1016/j.neucom.2023.126327
- [50] E. Hassan, M. Y. Shams, N. A. Hikal, and S. Elmougy, "The effect of choosing optimizer algorithms to improve computer vision tasks: a comparative study," Multimed Tools Appl, vol. 82, no. 11, pp. 16591–16633, May 2023, doi: 10.1007/s11042-022-13820-0
- [51] D. Lamani et al., "SVM directed machine learning classifier for human action recognition network," Scientific Reports, vol. 15, no. 1, Jan. 2025, doi: 10.1038/s41598-024-83529-7
- K.-L. Du, B. Jiang, J. Lu, J. Hua, and M. N. S. Swamy, "Exploring Kernel Machines and Support Vector Machines: Principles, Techniques, and Future Directions," Mathematics, vol. 12, no. 24, p. 3935, Dec. 2024, doi: 10.3390/math12243935
- [53] S. F. Hussain, "A novel robust kernel for classifying high-dimensional data using Support Vector Machines," Expert Systems with Applications, vol. 131, pp. 116-131, Oct. 2019, doi: 10.1016/j.eswa.2019.04.037

Vol. 6, No. 5, October 2025, Page. 3153-3172 P-ISSN: 2723-3863 https://jutif.if.unsoed.ac.id E-ISSN: 2723-3871 DOI: https://doi.org/10.52436/1.jutif.2025.6.5.5179

[54] J. Huo et al., "Comparison of KAN, MLP, and SVM for NIR Spectra Classification," in 2024 3rd International Conference on Automation, Robotics and Computer Engineering (ICARCE), China: IEEE, Dec. 2024, pp. 290–294. doi: 10.1109/ICARCE63054.2024.00060

- [55] M. -, A. Widodo, M. -, W. F. Mahmudy, and M. M. Arifin, "Comparison of Multi-layer Perceptron and Support Vector Machine Methods on Rainfall Data with Optimal Parameter Tuning," International Journal of Advanced Computer Science and Applications, vol. 14, no. 7, 2023, doi: 10.14569/IJACSA.2023.0140745
- [56] A. Jamali, S. K. Roy, D. Hong, P. M. Atkinson, and P. Ghamisi, "Spatial-Gated Multilayer Perceptron for Land Use and Land Cover Mapping," IEEE Geosci. Remote Sensing Lett., vol. 21, pp. 1–5, 2024, doi: 10.1109/LGRS.2024.3354175
- [57] Md. A. Fattah, S. R. Morshed, and S. Y. Morshed, "Multi-layer perceptron-Markov chain-based artificial neural network for modelling future land-specific carbon emission pattern and its influences on surface temperature," SN Appl. Sci., vol. 3, no. 3, p. 359, Feb. 2021, doi: 10.1007/s42452-021-04351-8